



Correlation between paraspinal muscle fat infiltration and thoracic vertebral degeneration based on phantom-less QCT: a novel insight into thoracic vertebral degeneration

Ziqi Jiang^{1,2} · Kexin Wang^{1,2} · Hongda Zhang^{2,3} · Yuanzhi Weng⁴ · Deming Guo^{1,2} · Chi Ma⁴ · Weijia William Lu⁴ · Hao Xu^{2,3} · Xiaoning Liu^{1,2}

Received: 19 October 2024 / Revised: 27 December 2024 / Accepted: 1 January 2025
© The Author(s), under exclusive licence to Springer-Verlag GmbH Germany, part of Springer Nature 2025

Abstract

Purpose This study aimed to elucidate the correlation between the degree of fat infiltration (FI) in thoracic paraspinal muscles and thoracic vertebral degeneration (TVD).

Methods This cross-sectional study comprised 474 patients who underwent standard thoracic computed tomography (CT) scans. The FI was quantified as the percentage of adipose tissues within the cross-sectional area of thoracic paraspinal muscles. Thoracic vertebra was assessed in terms of osteoporosis, ossification of the anterior longitudinal ligament (OALL), ossification of the posterior longitudinal ligament (OPLL), intervertebral disc calcification, intervertebral disc cavity, and facet joint osteoarthritis (FJO). Logistic regression, linear regression, subgroup, and receiver operating characteristic (ROC) analyses were assessed to evaluate the association between FI and TVD.

Results Multivariate logistic regression revealed that more severe FI was closely associated with more serious osteoporosis ($P < 0.001$). Furthermore, after adjusting for only age, higher FI was significantly associated with nastier FJO ($P < 0.05$). In male patients, severe FI was greatly associated with worse osteoporosis ($P < 0.05$). In female patients, severe FI maintained close correlations with more severe osteoporosis and FJO ($P < 0.05$). Furthermore, in patients aged < 60 or ≥ 60 years, higher FI had a strong correlation with more severe osteoporosis ($P < 0.001$). In patients aged < 60 years, higher FI was associated with worse intervertebral disc calcification, OALL, and FJO ($P < 0.05$). Meanwhile, in patients aged ≥ 60 years, increased FI was only associated with severe OPLL ($P < 0.05$). Multivariate linear regression showed that FI negatively correlated with bone mineral density in the general population and different sex and age groups ($P < 0.001$). ROC analysis indicated that FI could predict the occurrence of TVD ($P < 0.05$).

Conclusion Higher FI is associated with more severe TVD. Studies on TVD are currently limited; therefore, this study enriches the related research on TVD, and our findings would facilitate the early prediction and diagnosis of TVD in clinical practice. Furthermore, our findings indicate that thoracic spine pain (TSP) caused by TVD can be prevented, potentially improving the prognosis of patients with TSP.

Keywords Fat infiltration · Bone mineral density · Phantom-less quantitative computed tomography · Thoracic vertebral degeneration · Paraspinal muscles

Introduction

Thoracic spine pain (TSP) is a common condition that affects approximately 35.5% of the global population annually, with a prevalence ranging from 15.6 to 19.5% in adults and 13–35% in children and adolescents [1–3]. Severe TSP

may cause radiating rib pain, systemic discomfort, numbness, muscle weakness, and stiffness, significantly impacting daily life, work, and economic well-being [4–6]. Recent studies have shown that the current clinical management of TSP is limited and ambiguous; moreover, there are no clear indicators for early diagnosis [7]. This delay in diagnosis

Extended author information available on the last page of the article

adversely affects patients' quality of life. Therefore, this study innovatively proposed relevant diagnostic indicators for the early diagnosis of TSP related to thoracic vertebral degeneration (TVD).

TSP is a key manifestation of TVD, and is strongly linked to paravertebral muscle degeneration, which is quantifiable and has been shown to be a potential indicator for assessing TSP [8]. However, studies on TSP and its application in TVD are limited. Although traditionally magnetic resonance imaging (MRI) has been considered to be effective for fat infiltration (FI) assessment, current research has demonstrated that computed tomography (CT)-based FI assessment is no less effective than MRI evaluation [9]. FI was quantified as the percentage of adipose tissue within the cross-sectional area. Selecting the upper, middle, and lower levels for assessing paraspinal muscle FI corresponding to a specific vertebra has been reported to have good representativeness [10, 11]. The neuropeptides, cytokines, adipokines, and other inflammatory mediators that contribute to TSP and accelerate TVD may be produced and increase in quantity as FI escalates [12–15]. Additionally, since adipose tissue do not have the ability to contract, FI can severely impair the ability of paravertebral muscles to contract, further leading to TVD, and consequently TSP [16–18]. Therefore, investigating the relationship between FI and TVD will aid in the clinical treatment and prognosis of patients with TSP induced by TVD.

Extensive studies on lumbar and cervical spine conditions have revealed a strong link between vertebral degeneration and paraspinal muscle regression [10, 19–22]. Ossification of the anterior longitudinal ligament (OALL) and ossification of the posterior longitudinal ligament (OPLL) are typically degenerative diseases of the spine that affect the stability of spinal structures. OPLL is a common cause of spinal stenosis and spinal cord compression, which can lead to varying degrees of neurological symptom [23, 24]. Existing studies have shown that FJO induces TVD by affecting the mobility of the spine and then activating the compensatory role of paravertebral muscles in maintaining spinal stability [25]. At the thoracic level, thoracic paravertebral muscles play an important role in maintaining the biomechanical structure and normal physiological function of patients [26]. Spinal degeneration is complex. However, available studies have largely focused on the cervical and lumbar regions, with limited attention to the thoracic spine. Unlike other segments, the thoracic spine has restricted coronal movement due to the intervertebral and rib joints, and this may affect the causes and severity of TVD [27, 28]. However, available research have not adequately explored the connection between facet joint osteoarthritis (FJO), OALL, OPLL, intervertebral disc calcification, paraspinal

muscle FI, and intervertebral disc cavity (IDC), specifically in the thoracic spine.

This cross-sectional observational study aimed to evaluate the relationship between paraspinal muscle FI and TVD using several distinct degenerative indicators: osteoporosis, FJO, IDC, intervertebral disc calcification, OALL, and OPLL. In this study, osteoporosis was assessed using bone mineral density (BMD). Furthermore, this study sought to provide new insights and theoretical foundations for developing preventive and therapeutic strategies for TVD.

Methods

Patient population

This retrospective cross-sectional observational study reviewed the data of patients who underwent standard CT from 2021 to 2022. The inclusion criterion was patients with TSP who underwent thoracic spine CT. The exclusion criteria were as follows: (1) patients with thoracic surgery, vertebral fracture, or muscle tear (conditions that are associated with structural injury or anatomical damage resulting in inaccurate BMD and FI measurements); (2) patients with incomplete imaging data (the patient's anatomy could not be observed, resulting in an inability to make an accurate diagnosis). Data from the patients' clinical records included their age and sex. Based on the above criteria, 474 patients were included in the final analyses, as shown in Fig. 1. No patient dropped out of the study, as all data were derived from previous thoracic CT scans in this retrospective analysis.

Measurement of BMD and paravertebral muscle FI

BMD measurements in the thoracic spine (T10–T12) were conducted via CT scans using Phantom-less quantitative computed tomography (PL-QCT) [29]. An elliptical region of interest (ROI) was outlined in the vertebral body's internal space on axial CT images, avoiding the anterior cortical bone and posterior basivertebral veins. To reduce individual differences in ROI, two trained junior researchers delimited the ROI separately, and adjudication by an experienced researcher was solicited for ROIs with large range differences. We meticulously excluded any fractures or sclerotic areas from the ROI to ensure BMD accuracy, as illustrated in Fig. 2 (A, B, C). Vertebral levels with widespread sclerotic lesions, precluding accurate exclusion, were omitted from the analysis. Each intervertebral disc level's vertebral BMD was attributed to the BMD of the vertebra above it. Paravertebral muscle FI measurements were also performed with the same software, enabling manual muscle contour

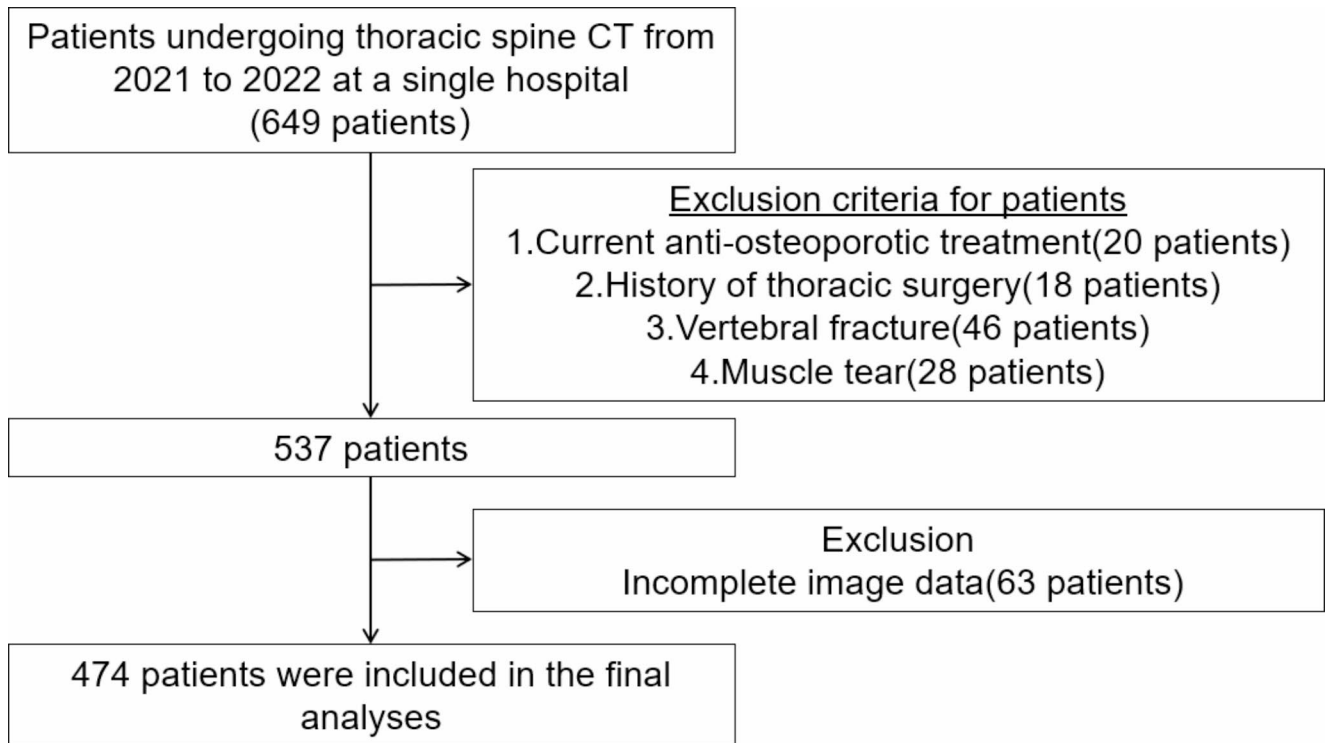


Fig. 1 Flow chart of the inclusion and exclusion process for this study

tracing and infiltration assessment. We classified BMD into three categories: normal bone mass ($\geq 120 \text{ g/cm}^3$), low bone mass ($80\text{--}120 \text{ g/cm}^3$), and osteoporosis ($\leq 80 \text{ g/cm}^3$), corresponding to none, slight-moderate, and severe labels [30].

Muscle FI was quantified across each vertebral body's upper, middle, and lower planes. We separately assessed the FI values for the erector spinae and multifidus muscles on both sides in each plane, as depicted in Fig. 3 (A, B). FI-T10, FI-T11, and FI-T12 represent the FI of paraspinal muscles measured at the corresponding vertebral levels for each patient, while average FI represents the mean FI of all measured paraspinal muscles. Two trained junior researchers who were blinded to the study's objectives conducted the BMD and FI measurements under the guidance of a board-certified radiologist with a decade of expertise in QCT analysis. By analyzing the reliability of FI measurements, moderate intraexaminer reliability (0.78) and moderate interexaminer reliability (0.71) were established. The reliability of BMD measurement was also verified with high intraexaminer reliability (0.94) and high interexaminer reliability (0.91).

Imaging diagnosis

The CT scans in this study were performed on a Neusoft GB18030 (NeuViz Peime 1.0) with scanning parameters set as follows: 120 kVp, 150 mAs/slice, 1.5 mm slice thickness,

and 512×512 matrix for chest CT; and 120 kVp, 150 mAs/slice, and 1024×1024 matrix for thoracic spine CT. The CT scans were performed on patients rather than healthy individuals, primarily to evaluate thoracic spine-related conditions or symptoms. A diagnostic committee composed of two senior radiologists and one senior orthopedic surgeon determined the study's related diagnoses. Due to the flexion, extension, and rotation of the spine, T10-T12 has greater mobility and mechanical vulnerability. Furthermore, T10-T12 also bears a higher the load than other parts of the thoracic spine, which could explain the higher frequency and severity of TVD in this region [24, 31]. To diagnose osteoarthritis in the facet joints, we first assessed the sagittal CT images of T10-T12, which is the first step in evaluating thoracic FJO. We modified the FJO classification criteria in this study based on the Weishaupt grading system [32] as follows: it was classified as none when the facet joint space was between 2 and 4 mm; slight-moderate when facet joint hypertrophy, osteophytes, and subchondral bone erosion were present; severe when there was critical facet joint space narrowing or severe osteophytes, facet joint hypertrophy, and subchondral bone erosion. Slight-moderate and severe cases were considered indicative of FJO, while none were regarded as normal.

The sagittal CT images of T10-T12 were evaluated to determine the presence of ossification in the anterior and posterior longitudinal ligaments. OPLL manifested as

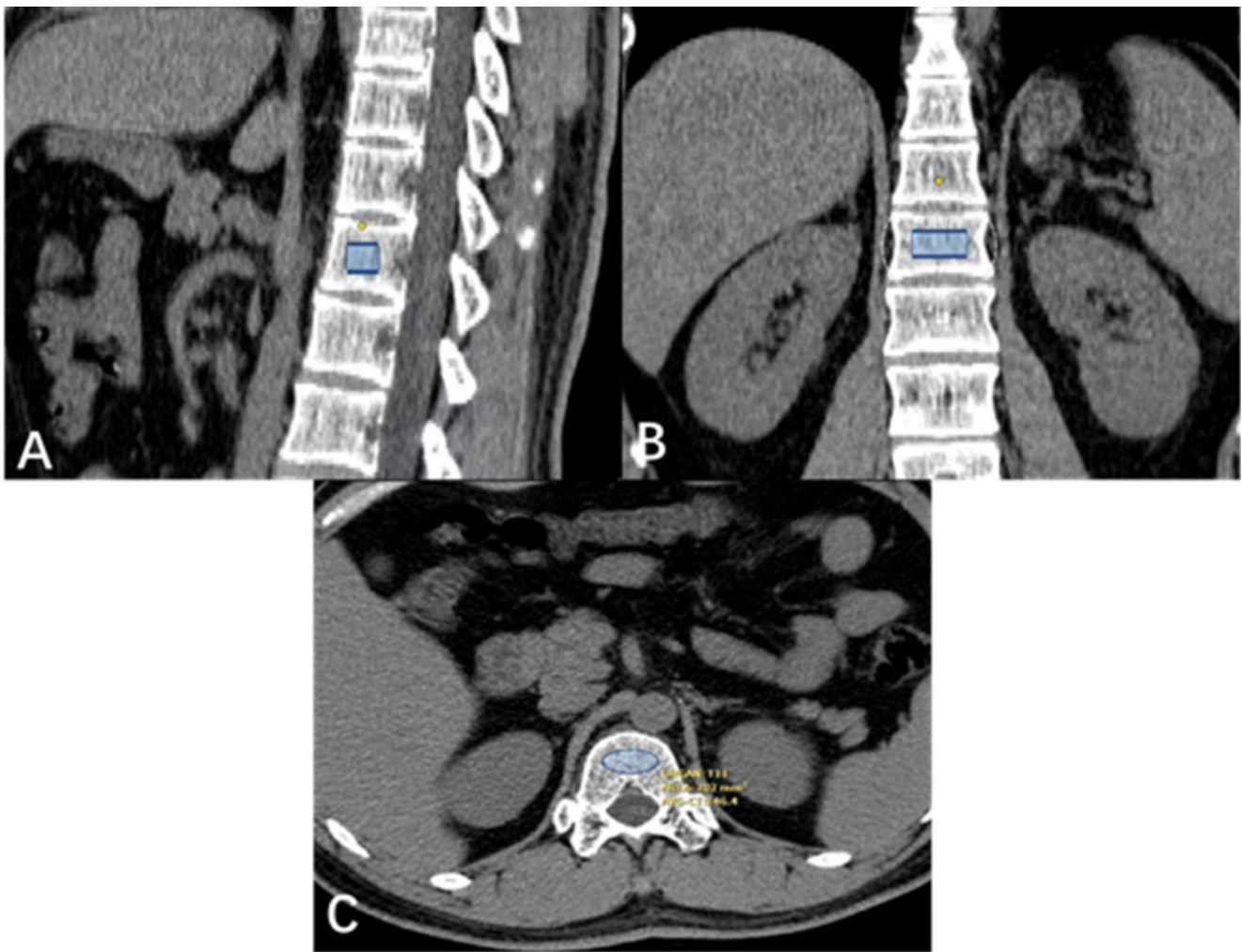


Fig. 2 Example of using software to measure BMD (A represents the range of BMD measurements in the sagittal plane, B indicates the range on the coronal plane, and C denotes the range on the axial plane). BMD, bone mineral density

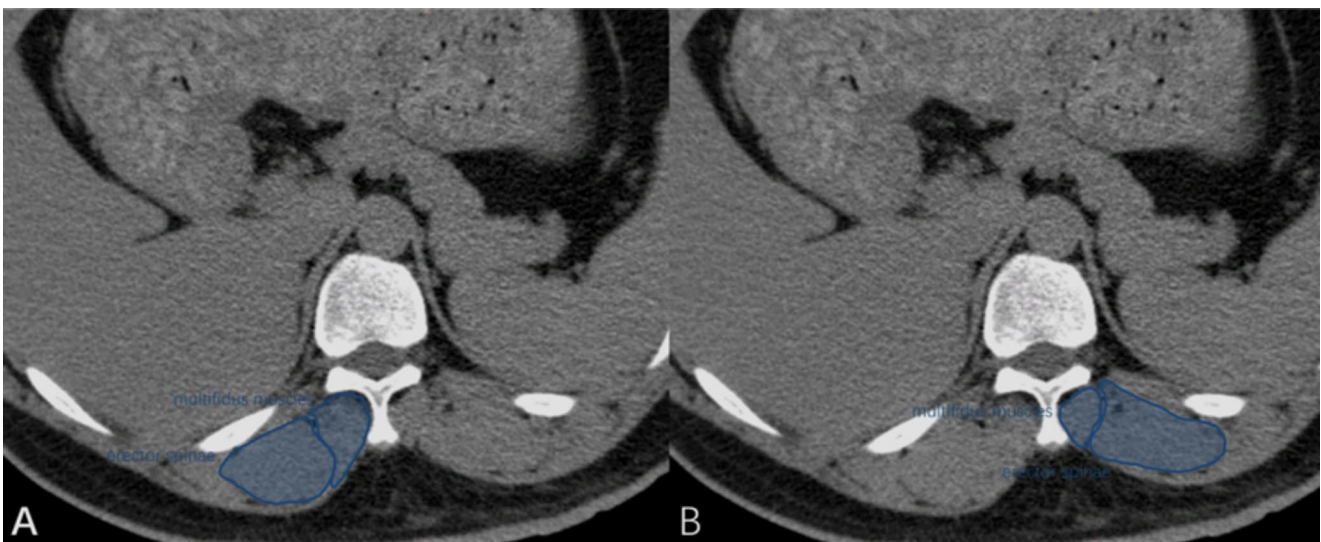


Fig. 3 Example of paravertebral muscle measurement in the thoracic spine (A corresponds to the patient's right side, B corresponds to the patient's left side, with 1 representing the multifidus muscle and 2 representing the erector spinae muscle)

papillary dense protrusion towards the spinal canal, causing deformation of the dural sac; OALL appeared as high-density patch-like areas on axial CT images. The presence of ligament ossification was regarded as positive, while the absence of ligament ossification was regarded as negative.

The classification criteria of the disc cavity were proposed by Lin et al. [33]. A positive diagnosis of disc cavity presence was made if irregular (or specific-shaped) low-density lesions were clearly visible within the intervertebral disc. If not, it was categorized as the lack of a disc cavity and assigned a negative value. Intervertebral disc calcification was determined as positive or negative based on whether distinct, irregular, high-density foci could be observed on imaging.

Statistical analysis

The SPSS version 25.0 (IBM Corp., Armonk, NY, USA) was used to evaluate the data statistically. With a confidence level of $1-\alpha=0.999$, sample sizes of $N_1=22.97$ and $N_2=5.61$, and a standard deviation (σ) of 11.64, the statistical power was calculated as >0.99 using PASS15. In this study, the variables adjusted in the multivariate analysis were those variables with P values <0.05 in the univariate analysis. Sex, age, and FI were continuous variables, while the indicators related to TVD were non-continuous variables. Logistic regression was used to adequately show their correlation. Univariate and multivariate logistic regression were used to analyze the correlations between sex, age, FI, and TVD. Linear regression analysis was deemed more suitable for evaluating both BMD and FI, as these are continuous variables. Linear regression analysis explored the correlation between the continuous variables BMD and FI. Finally, this study utilized ROC analysis to verify the predictive value. P value <0.05 was considered statistically significant.

Results

Univariate logistic regression analysis of TVD

As shown in Table 1, univariate logistic regression analysis revealed that higher age and FI were all closely associated with more severe TVD. However, sex was only significantly associated with osteoporosis and OALL ($P<0.05$).

Multivariate logistic regression analysis of paraspinal muscle FI and TVD

As shown in Table 2, multivariate logistic regression analysis revealed that after adjusting for age and sex, higher FI

was all closely associated with more severe osteoporosis ($P<0.001$). Specifically, for every 1-unit increase in T10-FI, the risk of osteoporosis increases by 8.6-12.0%; for every 1-unit increase in T11-FI, the risk of osteoporosis increases by 8.4-14.5%; for every 1-unit increase in T12-FI, the risk of osteoporosis increases by 8.2-14.3%; and for every 1-unit increase in average FI, the risk of osteoporosis increases by 9.2-14.8% ($P<0.001$). Furthermore, after adjusting for only age, higher FI was significantly associated with more critical FJO ($P<0.05$). For every 1-unit increasing in FI-T10, FI-T11, FI-T12, and average FI, the risk of FJO increased by 5.6%, 7.3%, 7.8%, and 7.2%, respectively ($P<0.05$).

Multivariate logistic regression analysis of paraspinal muscle FI and TVD in different genders

As shown in Table 3, multivariate logistic regression analysis in male patients revealed a significant association between higher FI and more severe osteoporosis ($P<0.05$). In female patients, higher FI was not only significantly associated with more severe osteoporosis ($P<0.05$) but also with worsening FJO ($P<0.05$).

Multivariate logistic regression analysis of paraspinal muscle FI and TVD in different age groups

As shown in Table 4, multivariate logistic regression analysis in patients aged <60 years and ≥ 60 years revealed that more severe FI was all closely associated with nastier osteoporosis ($P<0.001$). However, the associations of FI with intervertebral disc calcification, OALL, FJO, and OPLL showed differences between the age groups. In patients <60 years old, higher FI-T10, FI-T11, FI-T12, and average FI were closely associated with more serious intervertebral disc calcification, OALL, and FJO ($P<0.05$). Furthermore, in patients aged ≥ 60 years, severe FI-T10, FI-T11, FI-T12, and average FI were closely associated with worse OPLL ($P<0.05$).

Multivariate linear regression analysis of paraspinal muscle FI and BMD

As shown in Table 5, multivariate linear regression analysis, adjusted for age and sex, revealed that FI was negatively correlated with T10-BMD, T11-BMD, T12-BMD, and average BMD, respectively ($P<0.001$). In the subgroup analysis presented in Table 6, regardless of sex or age group (<60 years and ≥ 60 years), FI-T10, FI-T11, FI-T12, and average FI maintained negative linear correlations with T10-BMD, T11-BMD, T12-BMD, and average BMD, respectively ($P<0.001$).

Table 1 Univariate logistic regression analysis of TVD

	Sex		Female		FI-T10		FI-T11		FI-T12		FI-average	
	OR (95% CI)	<i>P</i> value										
Osteoporosis _{T10}	1.131 (1.098–1.165)	<0.001	3.201 (1.841–5.566)	<0.001	1.149 (1.112–1.188)	<0.001	1.195 (1.146–1.246)	<0.001	1.179 (1.132–1.229)	<0.001	1.183 (1.137–1.231)	<0.001
Osteoporosis _{T11}	1.141 (1.105–1.177)	< 0.001	2.893 (1.676–4.995)	<0.001	1.147 (1.110–1.185)	<0.001	1.166 (1.123–1.210)	<0.001	1.158 (1.115–1.202)	<0.001	1.166 (1.123–1.210)	<0.001
Osteoporosis _{T12}	1.135 (1.101–1.169)	< 0.001	3.298 (1.921–5.664)	<0.001	1.148 (1.111–1.187)	<0.001	1.165 (1.123–1.208)	<0.001	1.164 (1.120–1.210)	<0.001	1.168 (1.125–1.213)	<0.001
Osteoporosis ^a	1.135 (1.099–1.172)	< 0.001	3.203 (1.768–5.803)	<0.001	1.142 (1.106–1.178)	<0.001	1.151 (1.112–1.193)	<0.001	1.151 (1.109–1.194)	<0.001	1.156 (1.116–1.198)	<0.001
Osteoporosis ^b	1.135 (1.103–1.168)	< 0.001	3.454 (2.074–5.754)	<0.001	1.199 (1.150–1.249)	<0.001	1.240 (1.182–1.299)	<0.001	1.242 (1.182–1.304)	<0.001	1.242 (1.183–1.304)	<0.001
Intervertebral disc calcification _{T10–T12}	1.047 (1.027–1.067)	< 0.001	1.355 (0.825–2.225)	0.230	1.025 (1.009–1.041)	0.002	1.026 (1.008–1.044)	0.004	1.026 (1.007–1.045)	0.007	1.027 (1.009–1.045)	0.003
Intervertebral disc calcification _{T10–T11}	1.045 (1.018–1.073)	0.001	2.509 (1.186–5.308)	0.016	1.029 (1.010–1.048)	0.002	1.030 (1.009–1.051)	0.005	1.030 (1.008–1.052)	0.008	1.030 (1.010–1.051)	0.004
Intervertebral disc calcification _{T11–T12}	1.044 (1.022–1.066)	< 0.001	1.042 (0.598–1.816)	0.885	1.016 (0.998–1.034)	0.080	1.017 (0.997–1.037)	0.101	1.016 (0.994–1.037)	0.149	1.017 (0.997–1.037)	0.100
OALL _{T10–T12}	1.068 (1.050–1.088)	< 0.001	0.407 (0.268–0.620)	<0.001	1.036 (1.020–1.053)	<0.001	1.042 (1.023–1.061)	<0.001	1.047 (1.025–1.068)	<0.001	1.043 (1.023–1.062)	<0.001
OALL _{T10}	1.065 (1.045–1.086)	< 0.001	0.396 (0.248,0.630)	<0.001	1.033 (1.017–1.049)	<0.001	1.039 (1.020–1.058)	<0.001	1.043 (1.022–1.064)	<0.001	1.039 (1.020–1.058)	<0.001
OALL _{T11}	1.070 (1.048–1.092)	< 0.001	0.429 (0.267–0.689)	<0.001	1.038 (1.021–1.055)	<0.001	1.046 (1.026–1.066)	<0.001	1.049 (1.028–1.071)	<0.001	1.045 (1.026–1.065)	<0.001
OALL _{T12}	1.082 (1.056–1.109)	< 0.001	0.362 (0.208–0.631)	<0.001	1.041 (1.024–1.058)	<0.001	1.043 (1.024–1.063)	<0.001	1.053 (1.031–1.076)	<0.001	1.047 (1.027–1.067)	<0.001
OPLL _{T10–T12}	1.060 (1.017–1.105)	0.005	1.122 (0.411–3.065)	0.822	1.038 (1.015–1.061)	0.001	1.043 (1.019–1.068)	<0.001	1.047 (1.022–1.073)	<0.001	1.043 (1.019–1.068)	<0.001
OPLL _{T10}	1.079 (1.023–1.138)	0.005	1.537 (0.444–5.320)	0.498	1.031 (1.004–1.059)	0.025	1.034 (1.004–1.064)	0.024	1.038 (1.009–1.068)	0.011	1.035 (1.006–1.065)	0.017
OPLL _{T11}	1.057 (1.005–1.112)	0.033	0.867 (0.248–3.035)	0.823	1.042 (1.016–1.069)	0.001	1.051 (1.024–1.079)	<0.001	1.054 (1.026–1.083)	<0.001	1.050 (1.023–1.078)	<0.001
OPLL _{T12}	1.040 (0.983–1.100)	0.172	1.162 (0.257–5.249)	0.845	1.048 (1.019–1.077)	0.001	1.055 (1.025–1.086)	<0.001	1.058 (1.027–1.090)	<0.001	1.055 (1.025–1.086)	<0.001
IDC _{T10–T12}	1.069 (1.047–1.091)	< 0.001	0.867 (0.544–1.380)	0.547	1.032 (1.016–1.048)	< 0.001	1.037 (1.019–1.056)	<0.001	1.038 (1.018–1.058)	<0.001	1.037 (1.018–1.055)	<0.001
IDC _{T10–T11}	1.074 (1.046–1.103)	< 0.001	1.370 (0.745–2.518)	0.311	1.034 (1.016–1.051)	< 0.001	1.039 (1.020–1.059)	<0.001	1.038 (1.017–1.059)	<0.001	1.038 (1.019–1.058)	<0.001
IDC _{T11–T12}	1.056 (1.032–1.079)	< 0.001	0.728 (0.420–1.264)	0.260	1.027 (1.010–1.044)	0.001	1.033 (1.014–1.052)	0.001	1.035 (1.014–1.055)	0.001	1.032 (1.013–1.051)	0.001
FJO _{T10–T12}	1.145 (1.118–1.172)	< 0.001	1.156 (0.787–1.698)	0.461	1.268 (1.199–1.341)	< 0.001	1.302 (1.226–1.383)	<0.001	1.315 (1.235–1.400)	<0.001	1.309 (1.232–1.392)	<0.001

^a Osteoporosis assessed by the average BMD of T10–T12; ^b Osteoporosis assessed by any BMD of T10–T12. TVD, thoracic vertebral degeneration; FI, fat infiltration; OALL, ossification of the anterior longitudinal ligament; OPLL, ossification of the posterior longitudinal ligament; IDC, intervertebral disc cavity; FJO, facet joint osteoarthritis; OR, odds ratio; CI, confidence interval

Table 2 Multivariate logistic regression analysis of paraspinal muscle FI and TVD

	FI-T10		FI-T11		FI-T12		FI-average	
	OR (95% CI)	<i>P</i> value	OR (95% CI)	<i>P</i> value	OR (95% CI)	<i>P</i> value	OR (95% CI)	<i>P</i> value
Osteoporosis _{T10}	1.093 (1.056–1.130)	<0.001	1.120 (1.072–1.171)	<0.001	1.103 (1.058–1.151)	<0.001	1.114 (1.069–1.162)	<0.001
Osteoporosis _{T11}	1.091 (1.054–1.128)	<0.001	1.091 (1.0501.134)	<0.001	1.082 (1.041–1.124)	<0.001	1.094 (1.055–1.141)	<0.001
Osteoporosis _{T12}	1.086 (1.050–1.123)	<0.001	1.084 (1.044–1.025)	<0.001	1.082 (1.041–1.125)	<0.001	1.092 (1.051–1.135)	<0.001
Osteoporosis ^a	1.092 (1.057–1.130)	<0.001	1.085 (1.046–1.124)	<0.001	1.082 (1.042–1.124)	<0.001	1.096 (1.055–1.138)	<0.001
Osteoporosis ^b	1.120 (1.076–1.167)	<0.001	1.145 (1.090–1.203)	<0.001	1.143 (1.087–1.202)	<0.001	1.148 (1.193–1.205)	<0.001
Intervertebral disc calcification _{T10–T12}	1.006 (0.987–1.025)	0.539	1.004 (0.983–1.026)	0.688	1.003 (0.981–1.026)	0.776	1.005 (0.984–1.026)	0.652
Intervertebral disc calcification _{T10–T11}	1.016 (0.993–1.038)	0.175	1.015 (0.991–1.041)	0.222	1.014 (0.988–1.041)	0.290	1.016 (0.991–1.041)	0.213
Intervertebral disc calcification _{T11–T12}	0.994 (0.970–1.018)	0.616	1.072 (1.019–1.127)	0.007	0.990(0.961–1.109)	0.491	0.992 (0.965–1.019)	0.559
OALL _{T10–T12}	1.018 (0.998–1.038)	0.073	1.022 (0.999–1.045)	0.060	1.023 (0.999–1.048)	0.057	1.022 (0.999–1.045)	0.058
OALL _{T10}	1.018 (0.998–1.039)	0.073	1.025 (1.002–1.048)	0.033	1.026 (1.002–1.051)	0.036	1.024 (1.001–1.047)	0.041
OALL _{T11}	1.024 (1.003–1.045)	0.024	1.032 (1.008–1.056)	0.008	1.032 (1.007–1.058)	0.012	1.030 (1.007–1.055)	0.012
OALL _{T12}	1.031 (1.008–1.054)	0.008	1.031 (1.006–1.057)	0.016	1.041 (1.013–1.069)	0.004	1.035 (1.010–1.062)	0.007
OPLL _{T10–T12}	1.025 (0.997–1.052)	0.077	1.031 (1.003–1.059)	0.032	1.035 (1.006–1.064)	0.016	1.031 (1.003–1.060)	0.032
OPLL _{T10}	1.009 (0.973–1.047)	0.614	1.013 (0.975–1.052)	0.515	1.019 (0.983–1.056)	0.315	1.014 (0.977–1.053)	0.468
OPLL _{T11}	1.033 (1.003–1.064)	0.032	1.044 (1.014–1.075)	0.004	1.046 (1.015–1.079)	0.004	1.042 (1.011–1.074)	0.007
OPLL _{T12}	1.046 (1.013–1.080)	0.005	1.054 (1.020–1.089)	0.002	1.057 (1.022–1.094)	0.001	1.054 (1.020–1.089)	0.002
IDC _{T10–T12}	1.003 (0.984–1.022)	0.756	1.006 (0.986–1.027)	0.554	1.005 (0.984–1.027)	0.631	1.005 (0.980–1.026)	0.642
IDC _{T10–T11}	1.009 (0.988–1.030)	0.398	1.014 (0.992–1.037)	0.205	1.011 (0.987–1.035)	0.385	1.012 (0.989–1.035)	0.312
IDC _{T11–T12}	1.005 (0.985–1.026)	0.616	1.011 (0.990–1.033)	0.312	1.012 (0.989–1.035)	0.308	1.010 (0.988–1.032)	0.396
FJO _{T10–T12}	1.056 (1.005–1.110)	0.031	1.073 (1.013–1.137)	0.017	1.078 (1.015–1.145)	0.015	1.072 (1.012–1.136)	0.018

^a Osteoporosis assessed by the average BMD of T10-T12; ^b Osteoporosis assessed by any BMD of T10-T12; For osteoporosis and OALL, the multivariate logistic regression analysis adjusted for age and sex; while for intervertebral disc calcification, OPLL, IDC, and FJO, the multivariate logistic regression analysis adjusted for age only. TVD, thoracic vertebral degeneration; FI, fat infiltration; OALL, ossification of the anterior longitudinal ligament; OPLL, ossification of the posterior longitudinal ligament; IDC, intervertebral disc cavity; FJO, facet joint osteoarthritis; OR, odds ratio; CI, confidence interval

ROC analysis of paraspinal muscle FI for predicting TVD

As shown in Table 7, ROC analysis indicated that FI could predict the occurrence of TVD. In Figs. 4 and 5, the predictive value for osteoporosis was significantly higher than for intervertebral disc calcification, OALL, OPLL, IDC, and

FJO ($P < 0.05$). Additionally, the predictive value of FI for FJO was significantly higher than for other vertebral degeneration indicators except for osteoporosis ($P < 0.05$). Among all vertebral degeneration indicators, FI showed the highest predictive value for osteoporosis and the lowest for intervertebral disc calcification ($P < 0.05$).

Table 3 Multivariate regression analysis of paraspinal muscle FI and TVD in patients of different genders

		FI-T10		FI-T11		FI-T12		FI-average	
		OR (95% CI)	<i>P</i> value	OR (95% CI)	<i>P</i> value	OR (95% CI)	<i>P</i> value	OR (95% CI)	<i>P</i> value
Male	Osteoporosis _{T10}	1.158 (1.049–1.278)	0.004	1.318 (1.182–1.471)	<0.001	1.256 (1.107–1.426)	<0.001	1.303 (1.168–1.455)	<0.001
	Osteoporosis _{T11}	1.181 (1.068–1.306)	0.001	1.255 (1.120–1.407)	<0.001	1.246 (1.105–1.405)	<0.001	1.205 (1.109–1.409)	<0.001
	Osteoporosis _{T12}	1.188 (1.074–1.314)	0.001	1.238 (1.110–1.382)	<0.001	1.262 (1.118–1.425)	<0.001	1.252 (1.112–1.410)	<0.001
	Osteoporosis ^a	1.150 (1.039–1.274)	0.007	1.195 (1.070–1.335)	0.002	1.217 (1.072–1.381)	0.002	1.201 (1.064–1.355)	0.003
	Osteoporosis ^b	1.219 (1.100–1.350)	<0.001	1.315 (1.167–1.482)	<0.001	1.295 (1.147–1.462)	<0.001	1.308 (1.157–1.478)	<0.001
	Intervertebral disc calcification _{T10–T12}	0.946 (0.872–1.026)	0.179	0.939 (0.857–1.028)	0.174	0.960 (0.888–1.038)	0.305	0.945 (0.864–1.032)	0.209
	OALL _{T10–T12}	1.018 (0.977–1.059)	0.395	1.015 (0.974–1.058)	0.487	1.014 (0.972–1.057)	0.518	1.016 (0.974–1.060)	0.458
	OPLL _{T10–T12}	1.035 (0.997–1.074)	0.069	1.039 (0.999–1.080)	0.054	1.042 (1.000–1.085)	0.052	1.039 (0.999–1.080)	0.056
	IDC _{T10–T12}	1.030 (0.991–1.070)	0.132	1.021 (0.984–1.060)	0.264	1.037 (0.989–1.088)	0.134	1.030 (0.988–1.073)	0.165
	FJO _{T10–T12}	1.009 (0.937–1.087)	0.810	1.018 (0.933–1.110)	0.690	1.012 (0.933–1.098)	0.773	1.014 (0.932–1.102)	0.753
Female	Osteoporosis _{T10}	1.082 (1.043–1.122)	<0.001	1.092 (1.046–1.141)	<0.001	1.078 (1.032–1.126)	0.001	1.093 (1.047–1.141)	<0.001
	Osteoporosis _{T11}	1.076 (1.038–1.116)	<0.001	1.064 (1.025–1.104)	0.001	1.055 (1.015–1.097)	0.007	1.072 (1.030–1.117)	0.001
	Osteoporosis _{T12}	1.070 (1.032–1.109)	<0.001	1.057 (1.019–1.096)	0.003	1.053 (1.012–1.095)	0.010	1.066 (1.025–1.110)	0.002
	Osteoporosis ^a	1.083 (1.045–1.123)	<0.001	1.067 (1.029–1.107)	<0.001	1.062 (1.022–1.104)	0.002	1.079 (1.037–1.123)	<0.001
	Osteoporosis ^b	1.102 (1.055–1.151)	<0.001	1.101 (1.048–1.157)	<0.001	1.109 (1.052–1.169)	<0.001	1.115 (1.061–1.173)	<0.001
	Intervertebral disc calcification _{T10–T12}	1.017 (0.993–1.041)	0.165	1.016 (0.990–1.043)	0.239	1.013 (0.985–1.042)	0.370	1.016 (0.990–1.043)	0.229
	OALL _{T10–T12}	1.022 (0.999–1.046)	0.063	1.028 (1.001–1.055)	0.039	1.031 (1.002–1.060)	0.036	1.028 (1.001–1.056)	0.040
	OPLL _{T10–T12}	1.021 (0.981–1.062)	0.316	1.026 (0.984–1.070)	0.230	1.032 (0.990–1.077)	0.135	1.027 (0.985–1.072)	0.208
	IDC _{T10–T12}	0.992 (0.965–1.019)	0.544	1.001 (0.973–1.031)	0.924	0.990 (0.959–1.023)	0.552	0.994 (0.964–1.025)	0.697
	FJO _{T10–T12}	1.078 (1.005–1.155)	0.035	1.104 (1.015–1.199)	0.020	1.123 (1.025–1.230)	0.013	1.104 (1.015–1.201)	0.021

^a Osteoporosis assessed by the average BMD of T10–T12; ^b Osteoporosis assessed by any BMD of T10–T12; The multivariate logistic regression analysis adjusted for age. TVD, thoracic vertebral degeneration; FI, fat infiltration; OALL, ossification of the anterior longitudinal ligament; OPLL, ossification of the posterior longitudinal ligament; IDC, intervertebral disc cavity; FJO, facet joint osteoarthritis; OR, odds ratio; CI, confidence interval

Discussion

Our study delved into the complex and diverse causes of TSP, focusing on the link between paraspinal muscle FI and TVD. Univariate logistic regression analysis showed that FI was closely associated with TVD. Multivariate logistic regression analysis revealed that after adjusting for age and sex, FI was all closely associated with osteoporosis. Furthermore, after adjusting for age only, FI was significantly

associated with FJO. Moreover, multivariate logistic regression analysis of different ages revealed that FI was closely associated with osteoporosis. However, the associations of FI with intervertebral disc calcification, OALL, FJO, and OPLL showed differences between age groups. Subsequently, multivariate linear regression analysis, adjusted for age and sex, revealed that FI was negatively correlated with BMD. In the subgroup analysis, regardless of sex and age, FI maintained negative linear correlations with BMD. Finally, ROC analysis indicated that FI could predict the occurrence

Table 4 Multivariate regression analysis of paraspinal muscle FI and TVD in different age groups

		FI-T10		FI-T11		FI-T12		FI-average	
		OR (95% CI)	<i>P</i> value						
<60 years	Osteoporosis _{T10}	1.147 (1.081–1.216)	<0.001	1.167 (1.084–1.257)	<0.001	1.189 (1.103–1.282)	<0.001	1.180 (1.105–1.260)	<0.001
	Osteoporosis _{T11}	1.207 (1.113–1.308)	<0.001	1.184 (1.093–1.282)	<0.001	1.212 (1.117–1.315)	<0.001	1.208 (1.122–1.301)	<0.001
	Osteoporosis _{T12}	1.195 (1.107–1.291)	<0.001	1.174 (1.089–1.266)	<0.001	1.204 (1.113–1.303)	<0.001	1.207 (1.122–1.299)	<0.001
	Osteoporosis ^a	1.189 (1.103–1.281)	<0.001	1.165 (1.080–1.257)	<0.001	1.203 (1.109–1.304)	<0.001	1.203 (1.119–1.293)	<0.001
	Osteoporosis ^b	1.216 (1.118–1.323)	<0.001	1.203 (1.110–1.304)	<0.001	1.231 (1.131–1.340)	<0.001	1.229 (1.134–1.332)	<0.001
	Intervertebral disc calcification _{T10–T12}	1.061 (1.023–1.100)	0.001	1.072 (1.025–1.120)	0.002	1.079 (1.031–1.129)	0.001	1.073 (1.028–1.120)	0.001
	OALL _{T10–T12}	1.061 (1.023–1.100)	0.001	1.068 (1.023–1.115)	0.003	1.077 (1.030–1.126)	0.001	1.071 (1.027–1.118)	0.001
	OPLL _{T10–T12}	1.004 (0.917–1.098)	0.938	0.991 (0.870–1.129)	0.891	1.000 (0.881–1.136)	0.996	0.999 (0.891–1.120)	0.988
	IDC _{T10–T12}	1.027 (0.993–1.062)	0.120	1.036 (0.997–1.077)	0.700	1.051 (1.005–1.099)	0.029	1.037 (0.998–1.079)	0.065
	FJO _{T10–T12}	1.243 (1.155–1.337)	<0.001	1.268 (1.174–1.370)	<0.001	1.282 (1.182–1.390)	<0.001	1.282 (1.183–1.389)	<0.001
≥60 years	Osteoporosis _{T10}	1.091 (1.050–1.134)	<0.001	1.131 (1.073–1.191)	<0.001	1.096 (1.047–1.148)	<0.001	1.114 (1.061–1.169)	<0.001
	Osteoporosis _{T11}	1.076 (1.040–1.113)	<0.001	1.090 (1.046–1.136)	<0.001	1.070 (1.031–1.111)	<0.001	1.085 (1.043–1.129)	<0.001
	Osteoporosis _{T12}	1.073 (1.037–1.109)	<0.001	1.085 (1.042–1.130)	<0.001	1.071 (1.031–1.114)	<0.001	1.082 (1.040–1.126)	<0.001
	Osteoporosis ^a	1.081 (1.045–1.118)	<0.001	1.087 (1.045–1.130)	<0.001	1.073 (1.034–1.114)	<0.001	1.087 (1.046–1.130)	<0.001
	Osteoporosis ^b	1.107 (1.057–1.159)	<0.001	1.157 (1.089–1.230)	<0.001	1.135 (1.069–1.206)	<0.001	1.145 (1.079–1.216)	<0.001
	Intervertebral disc calcification _{T10–T12}	1.002 (0.980–1.024)	0.870	0.999 (0.974–1.025)	0.954	1.000 (0.974–1.026)	0.973	1.000 (0.976–1.025)	0.976
	OALL _{T10–T12}	1.026 (1.003–1.049)	0.028	1.030 (1.003–1.057)	0.027	1.032 (1.004–1.060)	0.023	1.030 (1.004–1.058)	0.024
	OPLL _{T10–T12}	1.038 (1.009–1.067)	0.009	1.044 (1.014–1.075)	0.004	1.046 (1.016–1.077)	0.003	1.044 (1.014–1.074)	0.004
	IDC _{T10–T12}	1.010 (0.991–1.030)	0.295	1.011 (0.990–1.033)	0.303	1.009 (0.987–1.032)	0.417	1.011 (0.999–1.033)	0.325
	FJO _{T10–T12}	1.061 (0.977–1.153)	0.161	1.082 (0.978–1.197)	0.128	1.067 (0.965–1.180)	0.204	1.075 (0.974–1.186)	0.152

^a Osteoporosis assessed by the average BMD of T10–T12; ^b Osteoporosis assessed by any BMD of T10–T12; For osteoporosis and OALL, the multivariate logistic regression analysis adjusted for sex; while for intervertebral disc calcification, OPLL, IDC, and FJO, the multivariate logistic regression analysis was not adjusted. TVD, thoracic vertebral degeneration; FI, fat infiltration; OALL, ossification of the anterior longitudinal ligament; OPLL, ossification of the posterior longitudinal ligament; IDC, intervertebral disc cavity; FJO, facet joint osteoarthritis; OR, odds ratio; CI, confidence interval

of TVD. The clinical management of TVD is still challenging; therefore, our study proposes early predictors for TVD. Our analyses were stratified by age and gender; hence, they can aid in early identification of high-risk groups of TVD, thereby effectively preventing the occurrence of adverse clinical events caused by TVD, such as fractures, and assist the current clinical management of TVD.

Our results were consistent with the findings of Chiapparelli et al., as FI showed a negative correlation with

lumbar spine BMD. However, this correlation differed at the femur, possibly reflecting different relationships between BMD and muscle FI across different anatomical regions [34]. Our study indirectly confirmed that the patterns of lumbar BMD and paravertebral muscle changes also apply to the thoracic spine [35]. TVD and muscle FI interact with each other, where the deterioration of either condition will lead to a corresponding worsening of the other. Factors such as muscle atrophy, deteriorating muscle quality, and

Table 5 Multivariate linear regression analysis of paraspinal muscle FI and BMD

	T10-BMD		T11-BMD		T12-BMD		BMD-average	
	β (95% CI)	<i>P</i> value						
FI-T10	-1.569 (-1.850, -1.287)	<0.001	-1.567(-1.848, -1.286)	<0.001	-1.581 (-1.868, -1.295)	<0.001	-1.572 (-1.847, -1.297)	<0.001
FI-T11	-1.775 (-2.085, -1.465)	<0.001	-1.776 (-2.085, -1.467)	<0.001	-1.793 (-2.108, -1.477)	<0.001	-1.781 (-2.083, -1.479)	<0.001
FI-T12	-1.736 (-2.069, -1.403)	<0.001	-1.736 (-2.068, -1.405)	<0.001	-1.785 (-2.122, -1.448)	<0.001	-1.752 (-2.076, -1.427)	<0.001
FI-average	-1.766 (-2.078, -1.454)	<0.001	-1.766 (-2.077, -1.456)	<0.001	-1.792 (-2.109, -1.475)	<0.001	-1.774 (-2.078, -1.470)	<0.001

The multivariate linear regression analysis adjusted for age and sex. FI, fat infiltration; BMD, bone mineral density; CI, confidence interval

Table 6 Stratified association between paraspinal muscle FI and BMD

		T10-BMD		T11-BMD		T12-BMD		BMD-average	
		β (95% CI)	<i>P</i> value						
Male	FI-T10	-1.623 (-2.151, -1.095)	<0.001	-1.551 (-2.085, -1.018)	<0.001	-1.607 (-2.148, -1.067)	<0.001	-1.594 (-2.110, -1.077)	<0.001
	FI-T11	-1.816 (-2.365, -1.266)	<0.001	-1.799 (-2.352, -1.247)	<0.001	-1.795 (-2.358, -1.231)	<0.001	-1.803 (-2.340, -1.267)	<0.001
	FI-T12	-1.840 (-2.406, -1.274)	<0.001	-1.766 (-2.338, -1.193)	<0.001	-1.785 (-2.367, -1.204)	<0.001	-1.797 (-2.351, -1.243)	<0.001
	FI-average	-1.801 (-2.354, -1.247)	<0.001	-1.745 (-2.303, -1.186)	<0.001	-1.770 (-2.338, -1.203)	<0.001	-1.772 (-2.313, -1.231)	<0.001
Female	FI-T10	-1.427 (-1.759, -1.096)	<0.001	-1.446 (-1.769, -1.122)	<0.001	-1.434 (-1.768, -1.101)	<0.001	-1.436 (-1.756, -1.115)	<0.001
	FI-T11	-1.627 (-2.000, -1.253)	<0.001	-1.623 (-1.989, -1.257)	<0.001	-1.645 (-2.020, -1.271)	<0.001	-1.631 (-1.992, -1.270)	<0.001
	FI-T12	-1.543 (-1.952, -1.135)	<0.001	-1.574 (-1.973, -1.175)	<0.001	-1.635 (-2.041, -1.229)	<0.001	-1.583 (-1.977, -1.189)	<0.001
	FI-average	-1.619 (-1.995, -1.242)	<0.001	-1.635 (-2.002, -1.267)	<0.001	-1.655 (-2.031, 1.279)	<0.001	-1.635 (-1.999, -1.272)	<0.001
<60 years	FI-T10	-3.486 (-3.955, -3.016)	<0.001	-3.513 (-3.982, -3.043)	<0.001	-3.553 (-4.037, -3.070)	<0.001	-3.518 (-3.979, -3.057)	<0.001
	FI-T11	-4.135 (-4.672, -3.598)	<0.001	-4.175 (-4.711, -3.639)	<0.001	-4.234 (-4.785, -3.683)	<0.001	-4.181 (-4.708, -3.655)	<0.001
	FI-T12	-4.893 (-5.475, -4.311)	<0.001	-4.934 (-5.515, -4.354)	<0.001	-5.021 (-5.617, -4.425)	<0.001	-4.948 (-5.516, -4.380)	<0.001
	FI-average	-4.256 (-4.784, -3.728)	<0.001	-4.293 (-4.819, -3.766)	<0.001	-4.354 (-4.896, -3.812)	<0.001	-4.301 (-4.817, -3.784)	<0.001
≥60 years	FI-T10	-1.135 (-1.460, -0.810)	<0.001	-1.137 (-1.462, -0.813)	<0.001	-1.157 (-1.486, -0.827)	<0.001	-1.143 (-1.459, -0.827)	<0.001
	FI-T11	-1.247 (-1.604, -0.889)	<0.001	-1.249 (-1.606, -0.893)	<0.001	-1.264 (-1.626, -0.901)	<0.001	-1.253 (-1.601, -0.906)	<0.001
	FI-T12	-1.121 (-1.498, -0.745)	<0.001	-1.124 (-1.500, -0.749)	<0.001	-1.173 (-1.553, -0.793)	<0.001	-1.139 (-1.505, -0.774)	<0.001
	FI-average	-1.217 (-1.574, -0.860)	<0.001	-1.220 (-1.576, -0.863)	<0.001	-1.248 (-1.609, -0.886)	<0.001	-1.228 (-1.575, -0.881)	<0.001

FI, fat infiltration; BMD, bone mineral density; CI, confidence interval

FI can lead to increased bone resorption, reduced trabecular bone volume, and diminished BMD [36]. There is also a mechanical coupling effect between muscles and bones. FI in muscles leads to reduced mechanical loading of skeletal muscles, which can trigger bone loss and decreased BMD. Meanwhile, muscle atrophy and FI may be related

to excessive autophagy, which can cause cellular stress and accelerate the loss of skeletal muscle mass [37]. Paraspinal muscles play a pivotal role in spinal stability, while spinal pathologies can alter these muscles' morphology, function, and biological characteristics [38]. Pain or limited mobility caused by spinal disorders may cause patients to reduce

Table 7 ROC analysis of paraspinal muscle FI for predicting TVD

	FI-T10			FI-T11			FI-T12			FI-average		
	specific cutoff values/ sensitivity/ specificity	AUC (95% CI)	<i>P</i> value	specific cutoff values/ sensitivity/ specificity	AUC (95% CI)	<i>P</i> value	specific cutoff values/ sensitivity/ specificity	AUC (95% CI)	<i>P</i> value	specific cutoff values/ sensitivity/ specificity	AUC (95% CI)	<i>P</i> value
Osteoporosis _{T10}	11.17/ 94.81/ 84.30	0.936 (0.910– 0.962)	<0.001	11.00/ 93.51/ 86.33/	0.942 (0.918– 0.967)	<0.001	9.50/ 94.81/ 82.28	0.930 (0.903– 0.958)	<0.001	10.61/ 97.40/ 84.56	0.942 (0.917– 0.967)	<0.001
Osteoporosis _{T11}	11.17/ 97.37/ 84.60	0.941 (0.915– 0.966)	<0.001	11.00/ 94.74/ 86.36/	0.939 (0.913– 0.964)	<0.001	8.67/ 96.05/ 77.78	0.925 (0.896– 0.953)	<0.001	10.61/ 97.37/ 84.34	0.940 (0.915– 0.966)	<0.001
Osteoporosis _{T12}	11.17/ 95.12 / 85.38	0.938 (0.913– 0.963)	<0.001	10.42/ 92.68/ 85.13	0.931 (0.906– 0.957)	<0.001	9.50/ 92.68/ 82.82	0.924 (0.897– 0.951)	<0.001	10.61/ 96.34/ 85.38	0.937 (0.912– 0.962)	<0.001
Osteoporosis ^a	11.25/ 95.45/ 82.51	0.942 (0.915– 0.970)	<0.001	11.67/ 90.91/ 86.45	0.933 (0.905– 0.961)	<0.001	11.17/ 90.91/ 85.47	0.927 (0.896– 0.957)	<0.001	10.94/ 95.45/ 84.24	0.940 (0.912– 0.968)	<0.001
Osteoporosis ^b	11.17/ 95.79/ 88.33	0.949 (0.928– 0.971)	<0.001	10.42/ 93.68/ 88.06	0.949 (0.927– 0.970)	<0.001	9.50/ 93.68/ 85.68	0.941 (0.918– 0.964)	<0.001	10.61/ 96.34/ 85.38	0.952 (0.931– 0.974)	<0.001
Intervertebral disc calci- fication _{T10–T12}	5.25/ 78.95/ 48.10	0.652 (0.592– 0.713)	<0.001	2.17/ 96.05/ 31.65	0.653 (0.593– 0.712)	<0.001	4.25/ 81.58/ 46.58	0.665 (0.608– 0.723)	<0.001	3.28/ 93.42/ 36.71	0.658 (0.599– 0.716)	<0.001
OALL _{T10–T12}	4.33/ 84.00/ 45.66	0.672 (0.621– 0.722)	<0.001	5.08/ 74.40/ 52.89	0.658 (0.606– 0.709)	<0.001	3.17/ 85.60/ 42.49	0.662 (0.611– 0.713)	<0.001	3.53/ 88.80/ 42.20	0.667 (0.617– 0.718)	<0.001
OPLL _{T10–T12}	9.08/ 68.75/ 65.71	0.683 (0.544– 0.823)	0.013	12.08/ 50.00/ 77.58	0.668 (0.523– 0.813)	0.022	9.00/ 68.75/ 68.57	0.690 (0.546– 0.833)	0.010	8.69/ 68.75/ 65.93	0.679 (0.536– 0.822)	0.015
IDC _{T10–T12}	4.67/ 93.10/ 47.66	0.728 (0.677– 0.778)	<0.001	3.25/ 94.25/ 40.36	0.715 (0.663– 0.767)	<0.001	4.08/ 93.10/ 49.22	0.725 (0.675– 0.775)	<0.001	4.50/ 90.80/ 47.40	0.726 (0.676– 0.777)	<0.001
FJO _{T10–T12}	5.75/ 71.75/ 85.81	0.844 (0.806– 0.883)	<0.001	3.25/ 84.76/ 71.61	0.843 (0.804– 0.882)	<0.001	3.33/ 81.90/ 72.90	0.840 (0.802– 0.879)	<0.001	2.94/ 88.89/ 68.39	0.849 (0.811– 0.887)	<0.001

^a Osteoporosis assessed by the average BMD of T10-T12; ^b Osteoporosis assessed by any BMD of T10-T12. TVD, thoracic vertebral degeneration; FI, fat infiltration; OALL, ossification of the anterior longitudinal ligament; OPLL, ossification of the posterior longitudinal ligament; IDC, intervertebral disc cavity; FJO, facet joint osteoarthritis; ROC, receiver operating characteristic; AUC, area under curve; CI, confidence interval

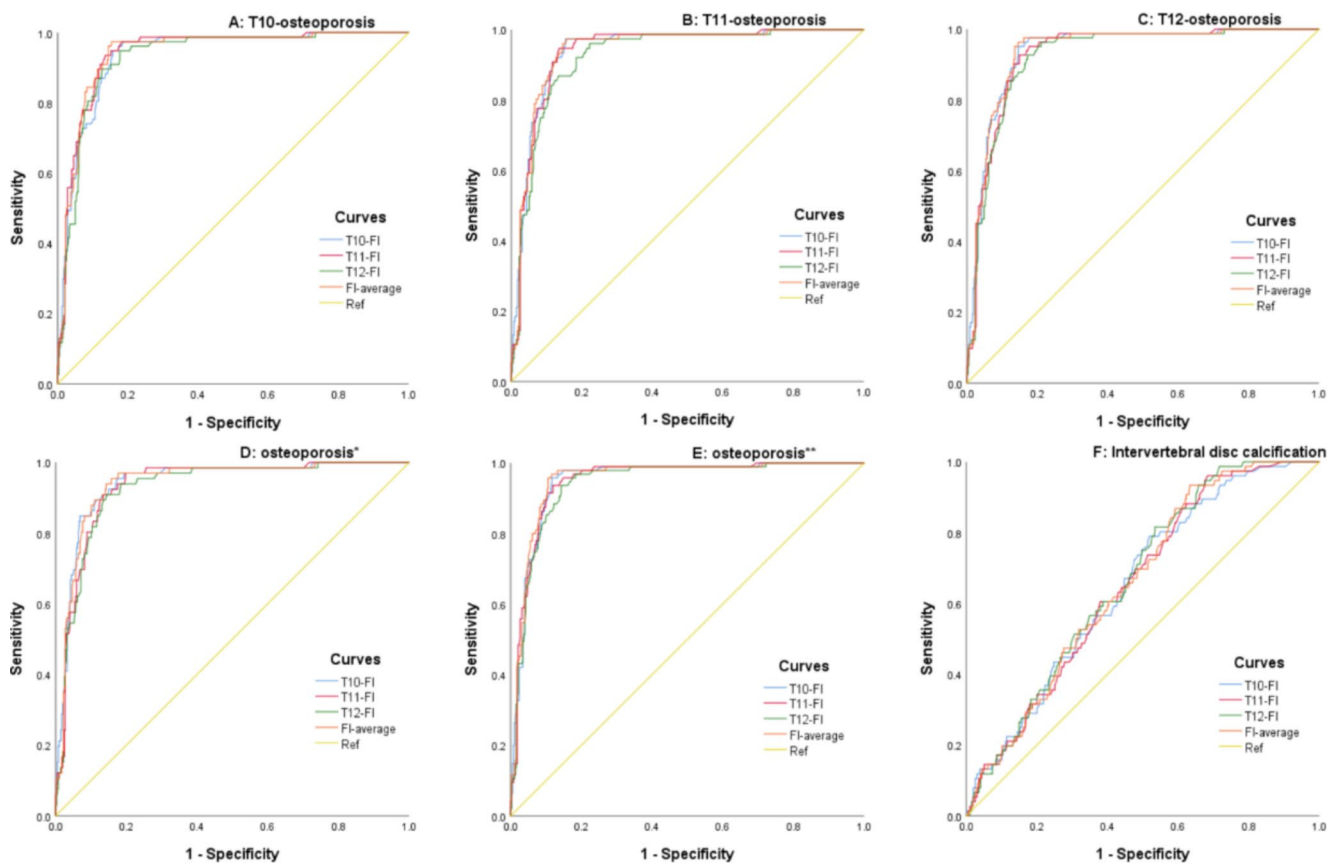


Fig. 4 ROC analysis of paraspinal muscle FI for predicting osteoporosis and intervertebral disc calcification

*Osteoporosis assessed by the average BMD of T10-T12; ** Osteoporosis assessed by any BMD of T10-T12;

their activity, resulting in disuse muscle atrophy. Degeneration alters spinal stability and biomechanical relationships, increases the load on intervertebral discs, and causes compensatory changes in paraspinal muscles, leading to load imbalance and subsequent atrophy [39].

Vertebral degeneration can lead to imbalances in paraspinal muscle volume and FI. This may be due to repetitive stress on the vertebrae from bone loss, prompting paraspinal muscle contractions to stabilize the lumbar region. Consequently, this increased muscle activity can enhance the susceptibility of lower-density vertebral bodies to fat degeneration [40]. Consistent with the findings of previous studies, our study identified a significant link between lumbar vertebral bone density and paraspinal muscle area and FI, suggesting that bone mineral loss is associated with paraspinal muscle degeneration, potentially contributing to low back pain [41]. Our multiple linear regression analysis pinpointed FI, which is inversely related to bone density, as a critical determinant of paraspinal muscle thoracic vertebral BMD. This underscores the importance of muscle structure and function for skeletal health. The study found a close correlation between paraspinal muscle FI and vertebral body degeneration. Although univariate logistic

regression analysis showed that all vertebral degeneration indicators were significantly associated with paraspinal muscle FI, multivariate logistic regression analysis revealed that paraspinal muscle FI was not closely correlated with intervertebral disc calcification, IDC, OALL, and some cases of OPLL. This contrasts with lumbar and cervical spine studies, which showed a stronger correlation between paraspinal muscle FI and intervertebral disc degeneration. These findings may be attributed to the unique anatomical features of the thoracic spine, such as smaller intervertebral discs and the orientation of facet and rib joints that limit disc herniation and overall spine mobility [42]. Additionally, fewer factors contribute to the degeneration of thoracic intervertebral discs compared to the cervical and lumbar spine [29], which can be considered one of the explanatory factors. Moreover, compared to the cervical spine, the limited mobility of the thoracic spine restricts the functions of the anterior longitudinal ligament and posterior longitudinal ligament to flexion and extension, resulting in less ligament calcification and a lower correlation with muscle FI.

Our analysis indicated that paraspinal muscle degeneration was more strongly associated with FJO than intervertebral disc degeneration or calcification of the

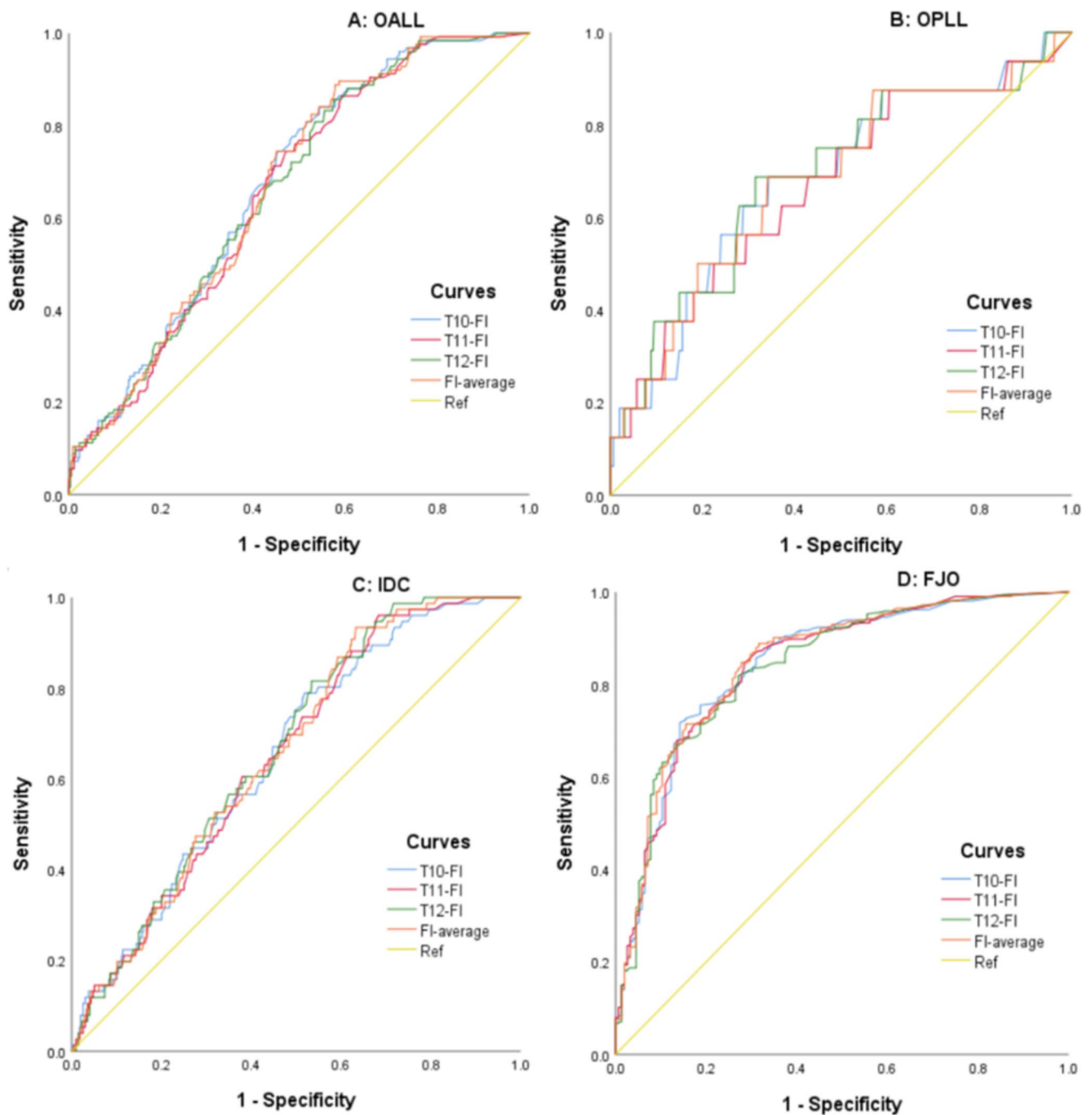


Fig. 5 ROC analysis of paraspinal muscle FI for predicting OALL, OPLL, IDC, and FJO
 FI, fat infiltration; OALL, ossification of the anterior longitudinal

ligament; OPLL, ossification of the posterior longitudinal ligament; IDC, intervertebral disc cavity; FJO, facet joint osteoarthritis; ROC, receiver operating characteristic

longitudinal ligaments. Patients with advanced FJO exhibited significantly higher muscle FI levels than those without the condition, implying that inflammation may accelerate the degenerative process. The inflammatory response from FJO can also lead to oxidative stress, hormone imbalances related to obesity, and adipocyte dysfunction within the adipose tissue. Additionally, FJO-related deformities and

functional impairments in adjacent spinal joints may disrupt normal spinal mechanics, potentially causing mechanical damage and adaptive changes in the surrounding adipose tissue [43].

This study relied solely on CT scan data to evaluate fat infiltration of the paraspinal muscles, which may have certain limitations in soft tissue resolution and fat tissue

detection. MRI, with its superior capability in detecting fat tissue and soft tissue abnormalities, especially in cases with significant fat infiltration, offers clear advantages [44]. Although MRI may have potential advantages in FI evaluation, current studies have confirmed that CT is not inferior to MRI in FI measurement [9].

This study has some limitations, including the following: (1) All patients in this study were outpatients who underwent thoracic CT scans during their visits; this limited the demographic information we could collect to age and gender. These data were included as adjustment variables in the multivariate analysis. However, since the patients did not undergo hospitalization or further systematic evaluations, other baseline information (e.g., weight, height, lifestyle factors, and comorbidities) was generally missing from outpatient records and could not be included in this study. (2) As a single-center study, the findings of this study are not generalizable to other countries, ethnic groups, and populations. (3) This research was a retrospective study, which could not be prospectively designed and could not track the historical data of the patients. Therefore, this study may be subject to certain data bias. Another limitation of this study is its retrospective design, as it relied solely on thoracic CT scans to evaluate bone density. Consequently, we were only able to analyze bone density changes in the thoracic region, without distinguishing between localized thoracic osteopenia and generalized osteoporosis. This limitation may have led to the inclusion of some patients with generalized osteoporosis, potentially influencing the results. Future prospective studies using diagnostic tools such as dual-energy X-ray absorptiometry or whole-body CT scans are needed to further differentiate between localized and generalized bone density changes and validate our findings.

Conclusion

Currently, regarding research on spinal diseases, studies on TVD are limited; this study fills the existing gap to a certain extent. Our study provides new insights into the relationship between TVD and paravertebral muscle FI, uncovering the close correlation between the degree of FI and various indicators of TVD. This study provides a new possibility for the early clinical prediction, prevention and improvement of the quality of life of TVD patients, and there is a possibility to improve the potential prognosis of patients with TSP.

Supplementary Information The online version contains supplementary material available at <https://doi.org/10.1007/s00586-025-08645-y>.

Author contributions Z.J. Conceptualization, Investigation, Data curation, Methodology, Software, Formal analysis, Visualization, Writing - original draft, Writing - review & editing. K.W., H.Z., Y. W., D.

G., C.M., W.L., H. X.: Conceptualization, Writing - review & editing. X. L.: Conceptualization, Validation, Funding acquisition, Project administration, Supervision. All authors read and approved the final manuscript.

Funding This study was funded by the 2023 Science and Technology Project of Jilin Provincial Department of Education (No. JJKH-20231226KJ).

Data availability No datasets were generated or analysed during the current study.

Declarations

Competing interests The authors declare no competing interests.

References

1. Parenteau CS, Lau EC, Campbell IC, Courtney A (2021) Prevalence of spine degeneration diagnosis by type, age, gender, and obesity using Medicare data. *Sci Rep* 11:5389. <https://doi.org/10.1038/s41598-021-84724-6>
2. Briggs AM, Smith AJ, Straker LM, Bragge P (2009) Thoracic spine pain in the general population: prevalence, incidence and associated factors in children, adolescents and adults. A systematic review. *BMC Musculoskelet Disord* 10:77. <https://doi.org/10.1186/1471-2474-10-77>
3. Kjaer P, Wedderkopp N, Korsholm L, Leboeuf-Yde C (2011) Prevalence and tracking of back pain from childhood to adolescence. *BMC Musculoskelet Disord* 12:98. <https://doi.org/10.1186/1471-2474-12-98>
4. Heneghan NR, Gormley S, Hallam C, Rushton A (2019) Management of thoracic spine pain and dysfunction: a survey of clinical practice in the UK. *Musculoskelet Sci Pract* 39:58–66. <https://doi.org/10.1016/j.msksp.2018.11.006>
5. Määttä J, Takatalo J, Leinonen T, Pienimäki T, Ylinen J, Häkkinen A (2022) Lower thoracic spine extension mobility is associated with higher intensity of thoracic spine pain. *J Man Manip Ther* 30:300–308. <https://doi.org/10.1080/10669817.2022.2047270>
6. Manchikanti L, Soin A, Benyamin RM, Singh V, Falco FJ, Calodney AK, Grami V, Hirsch JA (2018) An update of the systematic appraisal of the accuracy and utility of discography in chronic spinal pain. *Pain Phys* 21:91–110
7. Riseti M, Gambugini R, Testa M, Battista S (2023) Management of non-specific thoracic spine pain: a cross-sectional study among physiotherapists. *BMC Musculoskelet Disord* 24:398. <https://doi.org/10.1186/s12891-023-06505-8>
8. De Vitta A, Noll M, Monfort-Pañego M, Miñana-Signes V, Maciel NM (2023) Thoracic spine pain in high school adolescents: a one-year longitudinal study. *Healthc (Basel)* 11. <https://doi.org/10.3390/healthcare11020196>
9. Guo Z, Blake GM, Li K, Liang W, Zhang W, Zhang Y, Xu L, Wang L, Brown JK, Cheng X, Pickhardt PJ (2020) Liver fat content measurement with quantitative CT validated against MRI proton density fat fraction: a prospective study of 400 healthy volunteers. *Radiology* 294:89–97. <https://doi.org/10.1148/radiol.2019190467>
10. Kalichman L, Carmeli E, Been E (2017) The association between imaging parameters of the paraspinal muscles, spinal degeneration, and low back pain. *BioMed Res Int* 2017:2562957. <https://doi.org/10.1155/2017/2562957>

11. Cheng Z, Li Y, Li M, Huang J, Huang J, Liang Y, Lu S, Liang C, Xing T, Su K, Wen G, Zeng W, Huang L (2023) Correlation between posterior paraspinal muscle atrophy and lumbar intervertebral disc degeneration in patients with chronic low back pain. *Int Orthop* 47:793–801. <https://doi.org/10.1007/s00264-022-05621-9>
12. Fulgenzi CAM, D'Alessio A, Airolidi C, Scotti L, Demirtas CO, Gennari A, Cortellini A, Pinato DJ (2022) Comparative efficacy of novel combination strategies for unresectable hepatocellular carcinoma: a network meta-analysis of phase III trials. *Eur J Cancer* 174:57–67. <https://doi.org/10.1016/j.ejca.2022.06.058>
13. Noonan AM, Brown SHM (2021) Paraspinal muscle pathophysiology associated with low back pain and spine degenerative disorders. *JOR Spine* 4:e1171. <https://doi.org/10.1002/jsp2.1171>
14. Wang X, Jia R, Li J, Zhu Y, Liu H, Wang W, Sun Y, Zhang F, Guo L, Zhang W (2021) Research progress on the mechanism of Lumbarmultifidus injury and degeneration. *Oxid Med Cell Longev* 2021:6629037. <https://doi.org/10.1155/2021/6629037>
15. Zhu DC, Lin JH, Xu JJ, Guo Q, Wang YH, Jiang C, Lu HG, Wu YS (2021) An assessment of morphological and pathological changes in paravertebral muscle degeneration using imaging and histological analysis: a cross-sectional study. *BMC Musculoskelet Disord* 22:854. <https://doi.org/10.1186/s12891-021-04734-3>
16. MacDonald D, Moseley LG, Hodges PW (2009) Why do some patients keep hurting their back? Evidence of ongoing back muscle dysfunction during remission from recurrent back pain. *Pain* 142:183–188. <https://doi.org/10.1016/j.pain.2008.12.002>
17. MacDonald D, Moseley GL, Hodges PW (2010) People with recurrent low back pain respond differently to trunk loading despite remission from symptoms. *Spine* 35:818–824. <https://doi.org/10.1097/BRS.0b013e3181bc98f1>
18. Macdonald DA, Dawson AP, Hodges PW (2011) Behavior of the lumbar multifidus during lower extremity movements in people with recurrent low back pain during symptom remission. *J Orthop Sports Phys Ther* 41:155–164. <https://doi.org/10.2519/jospt.2011.3410>
19. Bendersky D, Asem M, Navarrete O (2022) Lumbar facet effusions and other degeneration parameters and its association with instability. *Neurol India* 70:S224–S229. <https://doi.org/10.4103/0028-3886.360912>
20. Ota Y, Connolly M, Srinivasan A, Kim J, Capizzano AA, Moritani T (2020) Mechanisms and origins of spinal pain: from molecules to anatomy, with diagnostic clues and imaging findings. *Radiographics* 40:1163–1181. <https://doi.org/10.1148/rg.2020190185>
21. Ekşi MŞ, Özcan-Ekşi EE (2024) Fatty infiltration of the erector spinae at the upper lumbar spine could be a landmark for low back pain. *Pain Pract* 24:278–287. <https://doi.org/10.1111/papr.13302>
22. Özcan-Ekşi EE, Ekşi MŞ, Akçal MA (2019) Severe lumbar intervertebral disc degeneration is associated with modic changes and fatty infiltration in the paraspinal muscles at all lumbar levels, except for L1-L2: a cross-sectional analysis of 50 symptomatic women and 50 age-matched symptomatic men. *World Neurosurg* 122:e1069–e1077. <https://doi.org/10.1016/j.wneu.2018.10.229>
23. Hirai T, Yoshii T, Nagoshi N, Takeuchi K, Mori K, Ushio S, Iwanami A, Yamada T, Seki S, Tsuji T, Fujiyoshi K (2018) Distribution of ossified spinal lesions in patients with severe ossification of the posterior longitudinal ligament and prediction of ossification at each segment based on the cervical OP index classification: a multicenter study (JOSL CT study). *BMC Musculoskelet Disord* 19:107. <https://doi.org/10.1186/s12891-018-2009-7>
24. Kim SI, Ha KY, Lee JW, Kim YH (2018) Prevalence and related clinical factors of thoracic ossification of the ligamentum flavum—a computed tomography-based cross-sectional study. *Spine J* 18:551–557. <https://doi.org/10.1016/j.spinee.2017.08.240>
25. Özcan-Ekşi EE, Börekci A, Ekşi MŞ (2023) Facet joint orientation/tropism could be associated with fatty infiltration in the lumbar paraspinal muscles. *World Neurosurg* 173:e606–e615. <https://doi.org/10.1016/j.wneu.2023.02.111>
26. Bogduk N, Macintosh JE, Pearcy MJ (1992) A universal model of the lumbar back muscles in the upright position. *Spine* 17:897–913. <https://doi.org/10.1097/00007632-199208000-00007>
27. Kadow T, Sowa G, Vo N, Kang JD (2015) Molecular basis of intervertebral disc degeneration and herniations: what are the important translational questions? *Clin Orthop Relat Res* 473:1903–1912. <https://doi.org/10.1007/s11999-014-3774-8>
28. Umezawa H, Daimon K, Fujiwara H, Nishiwaki Y, Michikawa T, Okada E, Nojiri K, Watanabe M, Katoh H, Shimizu K, Ishihama H (2022) Changes in cross-sectional areas of posterior extensor muscles in thoracic spine: a 10-year longitudinal MRI study. *Sci Rep* 12:14717. <https://doi.org/10.1038/s41598-022-19000-2>
29. Guo DM, Weng YZ, Yu ZH, Li SH, Qu WR, Liu XN, Qi H, Ma C, Tang XF, Li RY, Han Q, Xu H, Lu WW, Qin YG (2024) Semi-automatic proximal humeral trabecular bone density assessment tool: technique application and clinical validation. *Osteoporos Int* 35:1049–1059. <https://doi.org/10.1007/s00198-024-07047-y>
30. Subramaniam RM, Janowitz WR, Johnson GB, Lodge MA, Parisi MT, Ferguson MR, Hellinger JC, Gladish GW, Gupta NK (2017) ACR-SPR-STR practice parameter for the performance of cardiac positron emission tomography - computed tomography (PET/CT) imaging. *Clin Nucl Med* 42:918–927. <https://doi.org/10.1097/RLU.0000000000001827>
31. Murphy J, McLoughlin E, Davies AM, James SL, Botchu R (2020) Is T9-T11 the true thoracolumbar transition zone? *J Clin Orthop Trauma* 11:891–895. <https://doi.org/10.1016/j.jcot.2019.10.001>
32. Weishaupt D, Zanetti M, Boos N, Hodler J (1999) MR imaging and CT in osteoarthritis of the lumbar facet joints. *Skelet Radiol* 28:215–219. <https://doi.org/10.1007/s002560050503>
33. Lin J, Liu Z, Fu G, Zhang H, Chen C, Qi H, Jiang K, Zhang C, Ma C, Yang K, Wang C, Tan B, Zhu Q, Ding Y, Li C, Zheng Q, Cai D, Lu WW (2023) Distribution of bone voids in the thoracolumbar spine in Chinese adults with and without osteoporosis: a cross-sectional multi-center study based on 464 vertebrae. *Bone* 172:116749. <https://doi.org/10.1016/j.bone.2023.116749>
34. Chiapparelli E, Okano I, Adl Amini D, Zhu J, Salzmann SN, Tan ET, Moser M, Sax OC, Echeverri C, Oezel L, Shue J, Sama AA, Cammisia FP, Girardi FP, Hughes AP (2022) The association between lumbar paraspinal muscle functional cross-sectional area on MRI and regional volumetric bone mineral density measured by quantitative computed tomography. *Osteoporos Int* 33:2537–2545. <https://doi.org/10.1007/s00198-022-06430-x>
35. Zhao Y, Huang M, Ding J, Zhang X, Spuhler K, Hu S, Li M, Fan W, Chen L, Zhang X, Li S, Zhou Q, Huang C (2019) Prediction of abnormal bone density and osteoporosis from lumbar spine MR using modified Dixon quant in 257 subjects with quantitative computed tomography as reference. *J Magn Reson Imaging* 49:390–399. <https://doi.org/10.1002/jmri.26233>
36. Ma HT, Griffith JF, Xu L, Leung PC (2014) The functional muscle-bone unit in subjects of varying BMD. *Osteoporos Int* 25:999–1004. <https://doi.org/10.1007/s00198-013-2482-7>
37. Wilkinson DJ, Piasecki M, Atherton PJ (2018) The age-related loss of skeletal muscle mass and function: measurement and physiology of muscle fibre atrophy and muscle fibre loss in humans. *Ageing Res Rev* 47:123–132. <https://doi.org/10.1016/j.arr.2018.07.005>
38. Shahidi B, Parra CL, Berry DB, Hubbard JC, Gombatto S, Zlomislic V, Allen RT, Hughes-Austin J, Garfin S, Ward SR (2017) Contribution of lumbar spine pathology and age to paraspinal muscle size and fatty infiltration. *Spine* 42:616–623. <https://doi.org/10.1097/BRS.0000000000001848>

39. Xu X, Talifu Z, Zhang CJ, Gao F, Ke H, Pan YZ, Gong H, Du HY, Yu Y, Jing YL, Du LJ, Li JJ, Yang DG (2023) Mechanism of skeletal muscle atrophy after spinal cord injury: a narrative review. *Front Nutr* 10:1099143. <https://doi.org/10.3389/fnut.2023.1099143>
40. Cholewicki J, Simons AP, Radebold A (2000) Effects of external trunk loads on lumbar spine stability. *J Biomech* 33:1377–1385. [https://doi.org/10.1016/s0021-9290\(00\)00118-4](https://doi.org/10.1016/s0021-9290(00)00118-4)
41. Liu Z, Zhang Y, Huang D, Ma X, Duan Y, Jiang Y (2023) Quantitative study of vertebral body and paravertebral muscle degeneration based on dual-energy computed tomography: correlation with bone mineral density. *J Comput Assist Tomogr* 47:86–92. <https://doi.org/10.1097/RCT.0000000000001388>
42. Blumenkopf B (1988) Thoracic intervertebral disc herniations: diagnostic value of magnetic resonance imaging. *Neurosurgery* 23:36–40. <https://doi.org/10.1227/00006123-198807000-00008>
43. Fine N, Lively S, Séguin CA, Perruccio AV, Kapoor M, Ramper-saud R (2023) Intervertebral disc degeneration and osteoarthritis: a common molecular disease spectrum. *Nat Rev Rheumatol* 19:136–152. <https://doi.org/10.1038/s41584-022-00888-z>
44. Salimi H, Ohyama S, Terai H, Hori Y, Takahashi S, Hoshino M, Yabu A, Habibi H, Kobayashi A, Tsujio T, Kotake S, Nakamura H (2021) Trunk muscle mass measured by bioelectrical impedance analysis reflecting the cross-sectional area of the paravertebral muscles and back muscle strength: a cross-sectional analysis of a prospective cohort study of elderly population. *J Clin Med* 10. <https://doi.org/10.3390/jcm10061187>

Publisher's note Springer Nature remains neutral with regard to jurisdictional claims in published maps and institutional affiliations.

Springer Nature or its licensor (e.g. a society or other partner) holds exclusive rights to this article under a publishing agreement with the author(s) or other rightsholder(s); author self-archiving of the accepted manuscript version of this article is solely governed by the terms of such publishing agreement and applicable law.

Authors and Affiliations

Ziqi Jiang^{1,2} · Kexin Wang^{1,2} · Hongda Zhang^{2,3} · Yuanzhi Weng⁴ · Deming Guo^{1,2} · Chi Ma⁴ · Weijia William Lu⁴ · Hao Xu^{2,3} · Xiaoning Liu^{1,2}

✉ Xiaoning Liu
liuxy99@jlu.edu.cn

Ziqi Jiang
1287673682@qq.com

Kexin Wang
1287064651@qq.com

Hongda Zhang
hdzhang22@mails.jlu.edu.cn

Yuanzhi Weng
yzweng21@connect.hku.hk

Deming Guo
guodm91@jlu.edu.cn

Chi Ma
emma@hku.hk

Weijia William Lu
wwlu@hku.hk

Hao Xu
xuhao@jlu.edu.cn

¹ Second Hospital of Jilin University, Changchun, China

² Joint International Research Laboratory of Ageing Active Strategy and Bionic Health in Northeast Asia of Ministry of Education, changchun, China

³ Jilin University, Changchun, China

⁴ University of Hong Kong, Hong Kong, China